Supplemental Material

Multi-cell type gene co-expression network analysis reveals coordinated interferon response and cross cell-type correlations in systemic lupus erythematosus

Bharat Panwar[1]*, Benjamin J. Schmiedel[1], Shu Liang[1], Brandie White[1], Enrique Rodriguez[3], Kenneth Kalunian[2], Andrew J. McKnight[3], Rachel Soloff[3], Gregory Seumois[1], Pandurangan Vijayanand[1,2]*, Ferhat Ay[1,2]*

[1]La Jolla Institute for Immunology, La Jolla, California, USA.
[2]School of Medicine, University of California San Diego, La Jolla, California, USA.
[3]Kyowa Kirin Pharmaceutical Research, Inc., La Jolla, California, USA.

*co-corresponding authors: bpanwar@lji.org, vijay@lji.org, ferhatay@lji.org

SUPPLEMENTAL FIGURES

Figure S1

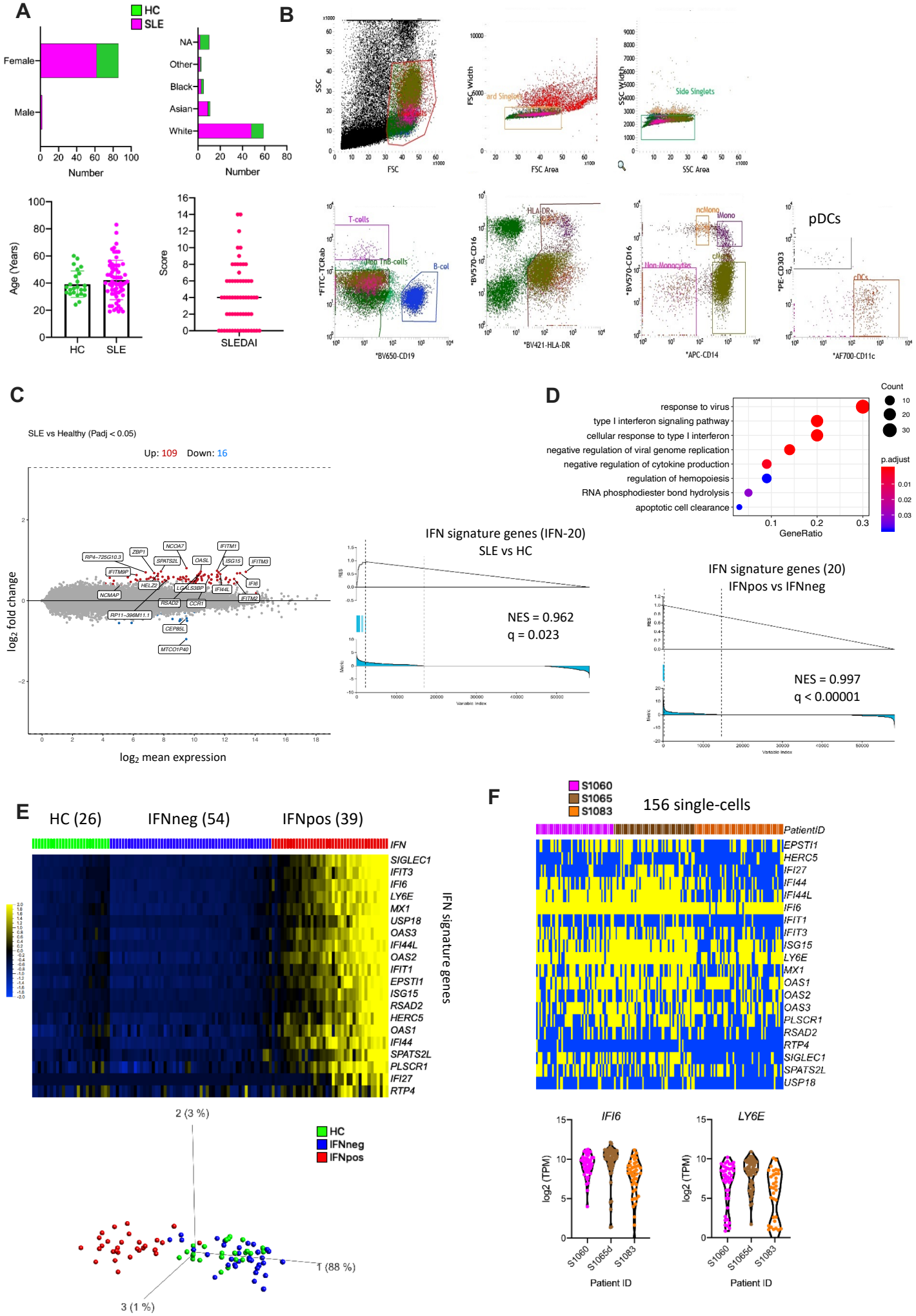
A
HC
SLE
Female
Male
Number
NA
Other
Black
Asian
White
Number
Age (Years)
HC
SLE
Score
SLEDAI
B
SSC
FSC
FSC Width
FSC Area
Side Singlets
SSC Width
SSC Area
T-cells
B-cel
*FITC-TCRab
*BV650-CD19
HLA-DR+
*BV570-CD16
*BV421-HLA-DR
ncMono
iMono
cMono
Non-Monocytes
*BV570-CD16
*APC-CD14
pDCs
*PE-CD303
*AF700-CD11c
C
SLE vs Healthy (Padj < 0.05)
Up: 109 Down: 16
log2 fold change
log2 mean expression
IFN signature genes (IFN-20)
SLE vs HC
NES = 0.962
q = 0.023
IFN signature genes (20)
IFNpos vs IFNneg
NES = 0.997
q < 0.00001
D
response to virus
type I interferon signaling pathway
cellular response to type I interferon
negative regulation of viral genome replication
negative regulation of cytokine production
regulation of hemopoiesis
RNA phosphodiester bond hydrolysis
apoptotic cell clearance
GeneRatio
Count
p.adjust
E
HC (26)
IFNneg (54)
IFNpos (39)
IFN
SIGLEC1
IFIT3
IFI6
LY6E
MX1
USP18
OAS3
IFI44L
OAS2
IFIT1
EPSTI1
ISG15
RSAD2
HERC5
OAS1
IFI44
SPATS2L
PLSCR1
IFI27
RTP4
IFN signature genes
2 (3 %)
1 (88 %)
3 (1 %)
HC
IFNneg
IFNpos
F
S1060
S1065
S1083
156 single-cells
PatientID
EPSTI1
HERC5
IFI27
IFI44
IFI44L
IFI6
IFIT1
IFIT3
ISG15
LY6E
MX1
OAS1
OAS2
OAS3
PLSCR1
RSAD2
RTP4
SIGLEC1
SPATS2L
USP18
IFI6
LY6E
log2 (TPM)
Patient ID
S1060
S1065d
S1083

Supplemental Figure S1. Transcription profile of classical monocytes reveals two molecular subtypes of SLE that shows stability in longitudinal data. (A) Different plots show the distribution of gender, ethnicity, age, and SLEDAI score in the SLE cohort. Healthy control (HC) samples are highlighted in green color and SLE samples are highlighted in magenta color (details in Supplemental Table S1). **(B)** Gating scheme of T-depleted PBMC for sorting of multiple immune cell types. Live cells were gated based on their forward side scatter versus side scatter profile followed by single cells gating by FSC then SSC and then finally according to their cell surface phenotype as follows, B cells ($CD19^+$, TCRa/b-), classical Mo (cMono, TCRa/b-, $CD19^-$, $HLA\text{-}DR^+$,$CD14^+$, $CD16^-$), intermediate Mo (iMono, TCRa/b-, $CD19^-$, $HLA\text{-}DR^+$, $CD16^+$, $CD14^+$), non-classical Mo (ncMono, TCRa/b-, $CD19^-$, $HLA\text{-}DR^+$, $CD16^+$ $CD14^{low}$), plasmacytoid dendritic cells (pDC, TCRa/b-, $CD19^-$, $HLA\text{-}DR^+$, $CD303^+$, $CD11c^-$) and conventional dendritic cells (cDC, TCRa/b-, $CD19^-$, $HLA\text{-}DR^+$, $CD303^-$, $CD11c^+$). **(C)** The MAplot shows 125 DEGs (P.adj < 0.05 from Benjamini-Hochberg test in DESeq2) between SLE and HC in classical monocytes. The top 20 genes (based on P.adj) are highlighted in boxes. The GSEA plot shows significant enrichment (NES=0.962; q=0.023) of 20 IFN-signature genes (IFN-20) in SLE vs HC. **(D)** Functional annotations (generated by clusterProfiler) of DEGs between IFNpos-vs-IFNneg (top). The color shows the significance (in terms of P.adj), the size is gene counts in annotation, and the X-axis shows gene ratio. The GSEA plot shows significant enrichment (NES=0.997; q<0.00001) of 20 IFN-signature genes (IFN-20) in IFNpos vs IFNneg comparison. **(E)** Expression of IFN-20 genes in all SLE patients (including longitudinal visits). Where each gene is presented as row-wise z-scores of transcripts per million (TPM) in IFNpos (red), IFNneg (blue) and HC (green); each column represents an individual patient and patients were clustered within their IFN status based on PC1 values (top). The PCA plot (bottom) shows the two molecular sub-types of SLE in different colors. Green, blue, and red represent HC, IFNneg and IFNpos, respectively (we used this color scheme in all figures). **(F)** The binary heatmap plot of single cell level expression of IFN-20 in cMo (156 cells) from three different IFNpos patients (shown in different colors in columns). In this binary heatmap, expression level of >1 TPM is highlighted in yellow and <1 TPM is shown in blue. The expression of two genes (*IFI6* and *LY6E*) is also provided as violin plots.

Figure S2

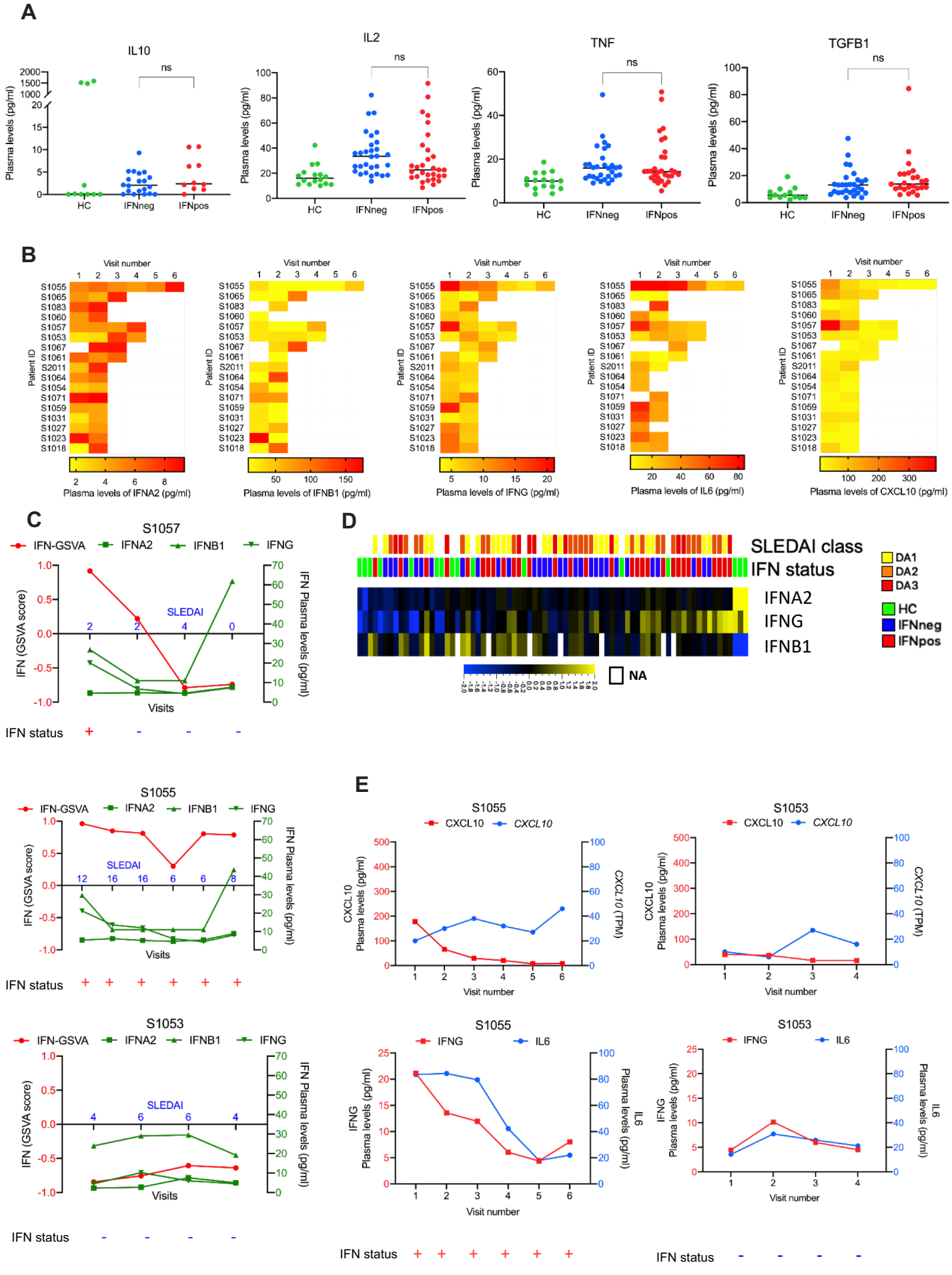
A
IL10
IL2
TNF
TGFB1
ns
Plasma levels (pg/ml)
HC
IFNneg
IFNpos
B
Visit number
Patient ID
Plasma levels of IFNA2 (pg/ml)
Plasma levels of IFNB1 (pg/ml)
Plasma levels of IFNG (pg/ml)
Plasma levels of IL6 (pg/ml)
Plasma levels of CXCL10 (pg/ml)
C
S1057
IFN-GSVA
IFNA2
IFNB1
IFNG
SLEDAI
IFN (GSVA score)
IFN Plasma levels (pg/ml)
Visits
IFN status
S1055
S1053
D
SLEDAI class
IFN status
DA1
DA2
DA3
HC
IFNneg
IFNpos
IFNA2
IFNG
IFNB1
NA
E
CXCL10
CXCL10 (TPM)
IFNG
IL6
Visit number

Supplemental Figure S2. Expression levels of different IFNs and cytokines in first and longitudinal visits. (A) Scatter dot-plots show plasma levels (pg/ml) of individual cytokines in HC, IFNneg and IFNpos SLE patients. Only first visit samples (n=76) were used in these scatter dot-plots. Differences between IFNpos and IFNneg were calculated using unpaired *t*-test (two-tailed) and statistical significance (p-value) levels are shown in each plot (ns: not significant, *: <0.05). **(B)** Series of heatmaps showing longitudinal information of different IFNs and pro-inflammatory cytokines (IL6 and CXCL10) in plasma. **(C)** Correlation between classical monocytes based IFN feature (GSVA score) and different IFN levels in plasma for three patients (S1057, S1055, and S1053). The SLEDAI score is also provided for each visit. **(D)** Heatmap of different IFN levels in plasma of SLE patients and healthy control. Where each IFN is presented as row-wise z-scores of IFN level in plasma (pg/ml) in IFNpos (red), IFNneg (blue) and HC (green); each column represents an individual patient. All patients are clustered based on PC1 values. The SLEDAI class panel shows SLEDAI score and is divided into three different categories based on score: DA1 (0-2), DA2 (3-7), and DA3 (>7) (yellow, orange and red, respectively). **(E)** Plots with connecting lines (upper and lower) show expression changes of multiple cytokines and chemokines in the longitudinal data for patient S1055 and S1053, where different analytes are plotted on different Y-axes (IFNG on Y1-axis in red color and IL6 on Y2-axis in blue color) in different colors (bottom graphs). The RNA-level expression of *CXCL10* is also shown (Y2-axis) with protein-level expression of CXCL10 (Y1-axis) (top graphs). The lower panel of bottom plots show their IFN response status over multiple longitudinal visits.

Figure S3

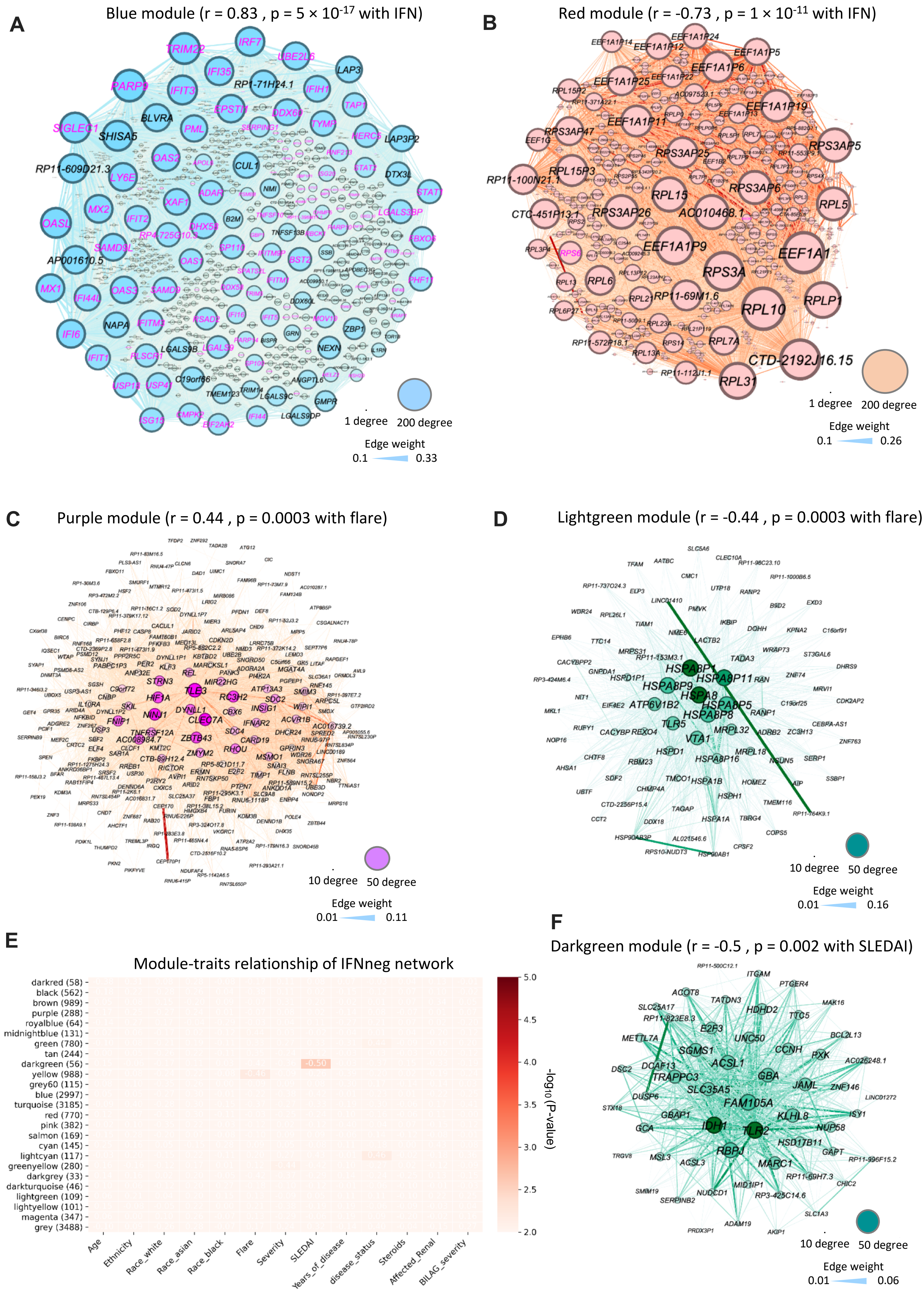
A
Blue module (r = 0.83 , p = 5 × 10-17 with IFN)
1 degree
200 degree
Edge weight
0.1
0.33
B
Red module (r = -0.73 , p = 1 × 10-11 with IFN)
1 degree
200 degree
Edge weight
0.1
0.26
C
Purple module (r = 0.44 , p = 0.0003 with flare)
10 degree
50 degree
Edge weight
0.01
0.11
D
Lightgreen module (r = -0.44 , p = 0.0003 with flare)
10 degree
50 degree
Edge weight
0.01
0.16
E
Module-traits relationship of IFNneg network
darkred (58)
black (562)
brown (989)
purple (288)
royalblue (64)
midnightblue (131)
green (780)
tan (244)
darkgreen (56)
yellow (988)
grey60 (115)
blue (2997)
turquoise (3185)
red (770)
pink (382)
salmon (169)
cyan (145)
lightcyan (117)
greenyellow (280)
darkgrey (33)
darkturquoise (46)
lightgreen (109)
lightyellow (101)
magenta (347)
grey (3488)
-0.50
-0.46
Age
Ethnicity
Race_white
Race_asian
Race_black
Flare
Severity
SLEDAI
Years_of_disease
disease_status
Steroids
Affected_Renal
BILAG_severity
-log10(P-value)
5.0
4.5
4.0
3.5
3.0
2.5
2.0
F
Darkgreen module (r = -0.5 , p = 0.002 with SLEDAI)
10 degree
50 degree
Edge weight
0.01
0.06

Supplemental Figure S3. Interesting modules from SLE and IFNneg patients based WGCNA network. Gephi based visualization of the blue module **(A)** and red module **(B)**, where nodes are sized according to the number of edges (connections), and the edge thickness is proportional to the strength of co-expression. Available IFN related genes (IFN-363) are highlighted in magenta colors. Similarly, purple **(C)** and lightgreen **(D)** modules from SLE network are also visualized by Gephi. **(E)** The module-traits correlation matrix heatmap of WGCNA based on total 25 different modules and external clinical features such as age, ethnicity, flare, severity etc from IFNneg patients. The color shows significance ($-Log_{10}$ of p-value) and Spearman's correlation values are provided in the heatmap. We only show the p-value for modules with significant correlation (p-value < 0.01). The number of genes in each module is also shown (in brackets) with the module name. **(F)** Gephi based visualization of the darkgreen module from IFNneg network, where nodes are sized according to the number of edges (connections), and the edge thickness is proportional to the strength of co-expression.

Figure S4

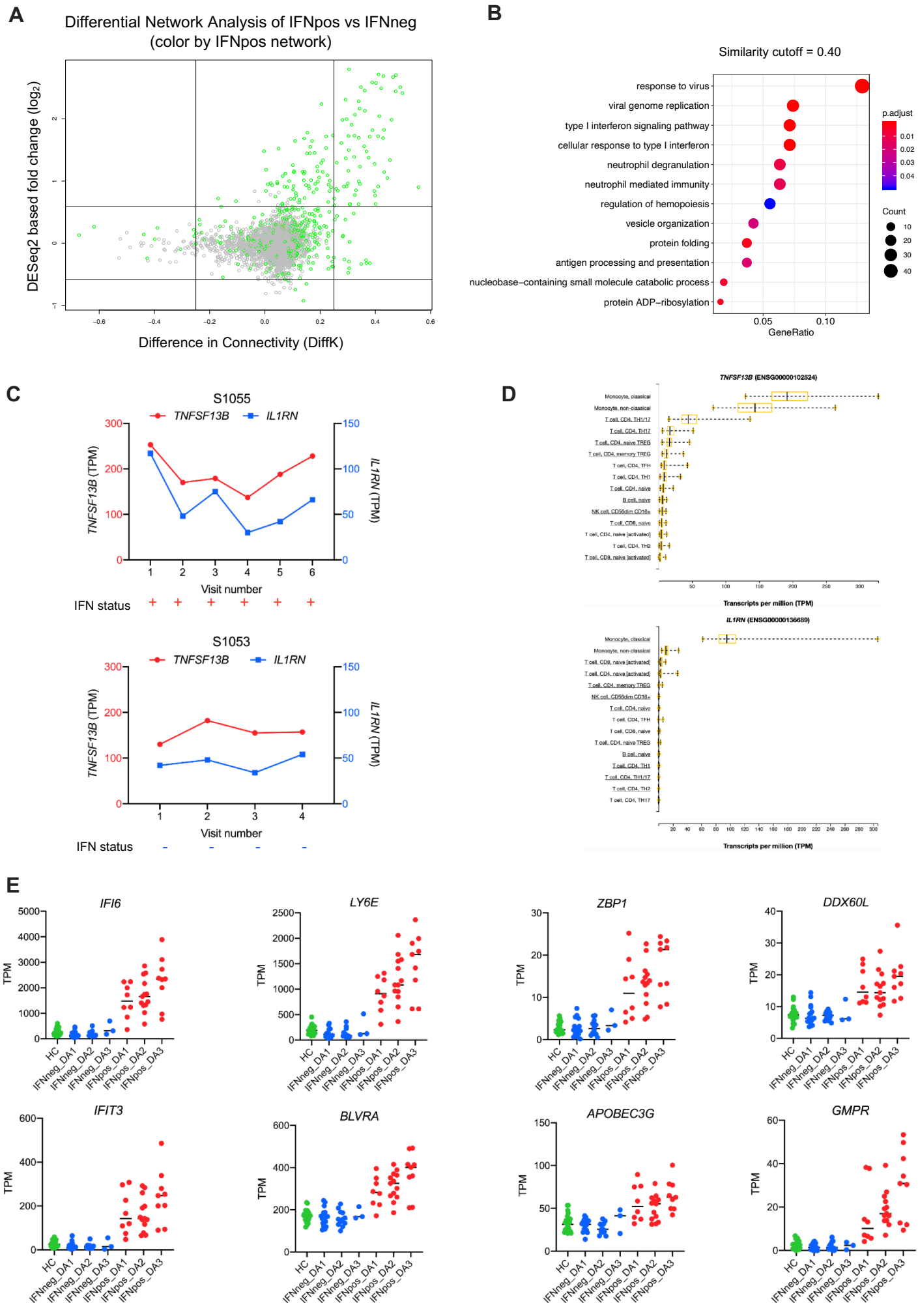
A
Differential Network Analysis of IFNpos vs IFNneg
(color by IFNpos network)
DESeq2 based fold change (log2)
Difference in Connectivity (DiffK)
B
Similarity cutoff = 0.40
response to virus
viral genome replication
type I interferon signaling pathway
cellular response to type I interferon
neutrophil degranulation
neutrophil mediated immunity
regulation of hemopoiesis
vesicle organization
protein folding
antigen processing and presentation
nucleobase−containing small molecule catabolic process
protein ADP−ribosylation
p.adjust
Count
GeneRatio
C
S1055
TNFSF13B
IL1RN
TNFSF13B (TPM)
IL1RN (TPM)
Visit number
IFN status
S1053
D
TNFSF13B (ENSG00000102524)
IL1RN (ENSG00000136689)
Transcripts per million (TPM)
E
IFI6
LY6E
ZBP1
DDX60L
IFIT3
BLVRA
APOBEC3G
GMPR
TPM
HC
IFNneg_DA1
IFNneg_DA2
IFNneg_DA3
IFNpos_DA1
IFNpos_DA2
IFNpos_DA3

Supplemental Figure S4. Combined analysis of differential network and gene expression of classical monocytes reveals two known immune modulators (*TNFSF13B* and *IL1RN*) and whose expression is dysregulated in SLE. (A) The plot shows both differentially expressed (DEGs) and connected genes (DCGs) from the IFNpos network based green and grey modules only. Where the X-axis is the difference in the connectivity (DiffK = K1-K2; K1=connectivity in IFNpos network; K2=connectivity in IFNneg network) and the Y-axis is the DESeq2 based fold-change (log_2). By default, the 'grey' module is generated by WGCNA for non-co-expressed genes so it shows that green module genes are well-expressed as well as well-connected in the IFNpos in comparison to grey module genes. **(B)** Functional annotations (generated by clusterProfiler) from all green module genes in IFNpos network. The color shows the significance (in terms of P.adj), the size is gene counts in annotation, and the X-axis shows gene ratio. **(C)** Expression changes of *TNFSF13B* (*BAFF)* and *IL1RN* in longitudinal data from patients S1057 and S1053, where genes are plotted on different Y-axes; *TNFSF13B* on Y1-axis in red and *IL1RN* on Y2-axis in blue. The lower panel of this plot shows corresponding IFN response status over multiple longitudinal visits. **(D)** The DICE database-based expression of *TNFSF13B* and *IL1RN* in different immune cell types from healthy donors. Where X-axis is expression (TPM) level and Y-axis shows different immune cell types. **(E)** The individual expression plot of genes of interest from the green module using IFN response status as well as SLEDAI categories.

Figure S5

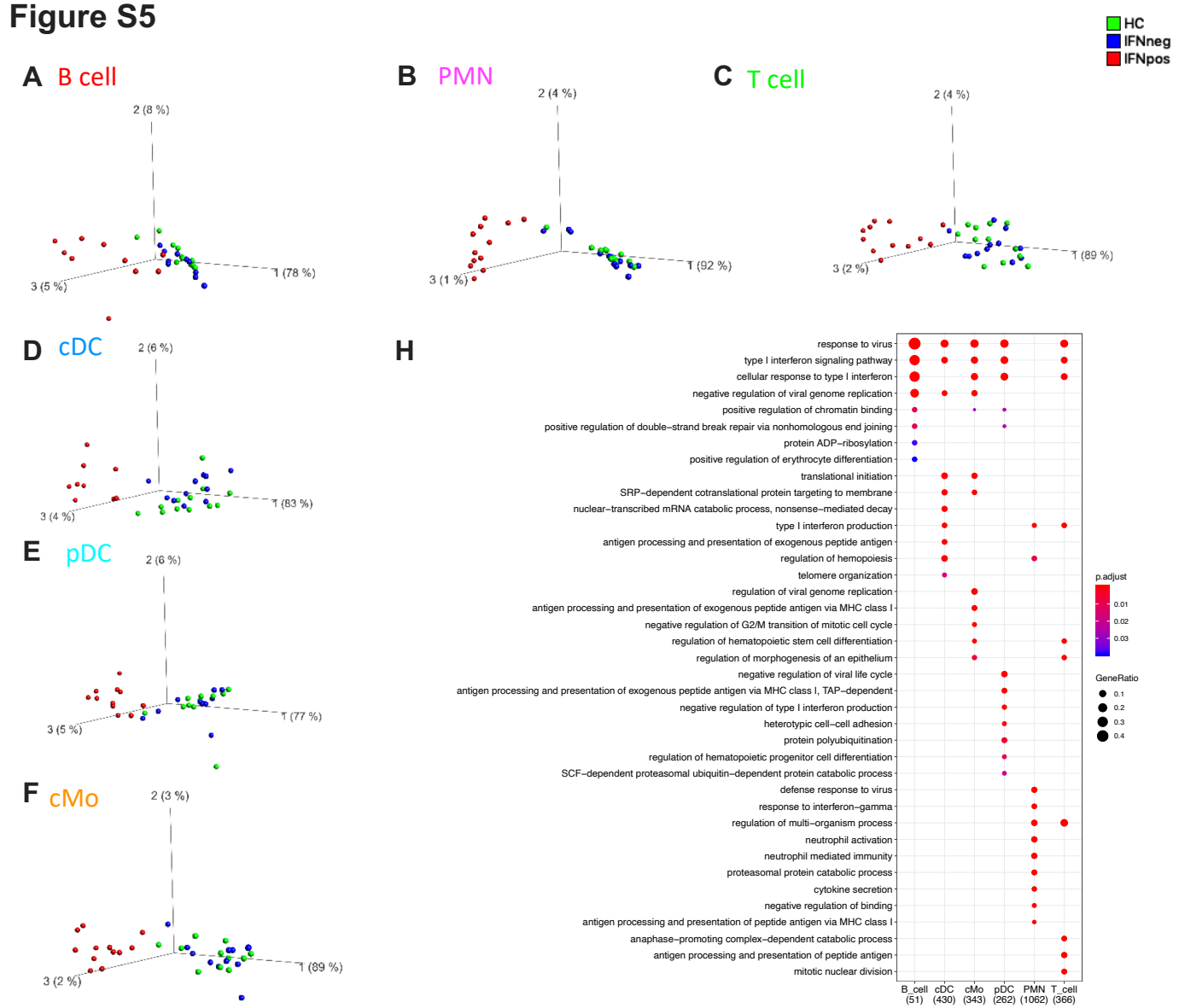
HC
IFNneg
IFNpos
A B cell
2 (8 %)
1 (78 %)
3 (5 %)
B PMN
2 (4 %)
1 (92 %)
3 (1 %)
C T cell
2 (4 %)
1 (89 %)
3 (2 %)
D cDC
2 (6 %)
1 (83 %)
3 (4 %)
E pDC
2 (6 %)
1 (77 %)
3 (5 %)
F cMo
2 (3 %)
1 (89 %)
3 (2 %)
H
response to virus
type I interferon signaling pathway
cellular response to type I interferon
negative regulation of viral genome replication
positive regulation of chromatin binding
positive regulation of double−strand break repair via nonhomologous end joining
protein ADP−ribosylation
positive regulation of erythrocyte differentiation
translational initiation
SRP−dependent cotranslational protein targeting to membrane
nuclear−transcribed mRNA catabolic process, nonsense−mediated decay
type I interferon production
antigen processing and presentation of exogenous peptide antigen
regulation of hemopoiesis
telomere organization
regulation of viral genome replication
antigen processing and presentation of exogenous peptide antigen via MHC class I
negative regulation of G2/M transition of mitotic cell cycle
regulation of hematopoietic stem cell differentiation
regulation of morphogenesis of an epithelium
negative regulation of viral life cycle
antigen processing and presentation of exogenous peptide antigen via MHC class I, TAP−dependent
negative regulation of type I interferon production
heterotypic cell−cell adhesion
protein polyubiquitination
regulation of hematopoietic progenitor cell differentiation
SCF−dependent proteasomal ubiquitin−dependent protein catabolic process
defense response to virus
response to interferon−gamma
regulation of multi−organism process
neutrophil activation
neutrophil mediated immunity
proteasomal protein catabolic process
cytokine secretion
negative regulation of binding
antigen processing and presentation of peptide antigen via MHC class I
anaphase−promoting complex−dependent catabolic process
antigen processing and presentation of peptide antigen
mitotic nuclear division
B_cell (51)
cDC (430)
cMo (343)
pDC (262)
PMN (1062)
T_cell (366)
p.adjust
0.01
0.02
0.03
GeneRatio
0.1
0.2
0.3
0.4
G
IFN
HC
IFNneg
IFNpos
2.0
1.8
1.6
1.4
1.2
1.0
0.8
0.6
0.4
0.2
0.0
-0.2
-0.4
-0.6
-0.8
-1.0
-1.2
-1.4
-1.6
-1.8
-2.0
NA
cMo
T cell
PMN
pDC
cDC
B cell
HERC5
IFI6
IFI44
IFI44L
IFIT3
ISG15
MX1
OAS3
PLSCR1
RSAD2
IFI27
IFIT1
SIGLEC1
USP18
SPATS2L
OAS2
RTP4
OAS1
EPSTI1
LY6E
IFN signature genes

Supplemental Figure S5. IFN-based molecular signature is independent of immune cell types. **(A-F)** PCA plots of different cell types based on IFN signature genes (IFN-20). **(G)** Expression of IFN-20 genes presented as row-wise z-scores of TPM in IFNpos (red), IFNneg (blue) and HC (green) for each cell type separately. The expression profile is absent (used blank or 'NA') for a few patients in some cell types. Patients were clustered within their IFN status based on PC1 values. **(H)** Functional annotations (generated by clusterProfiler) of all DEGs (IFNpos-vs-IFNneg) from different cell types. The color shows the significance (in terms of P.adj) and the size is gene ratio of annotations.

Figure S6

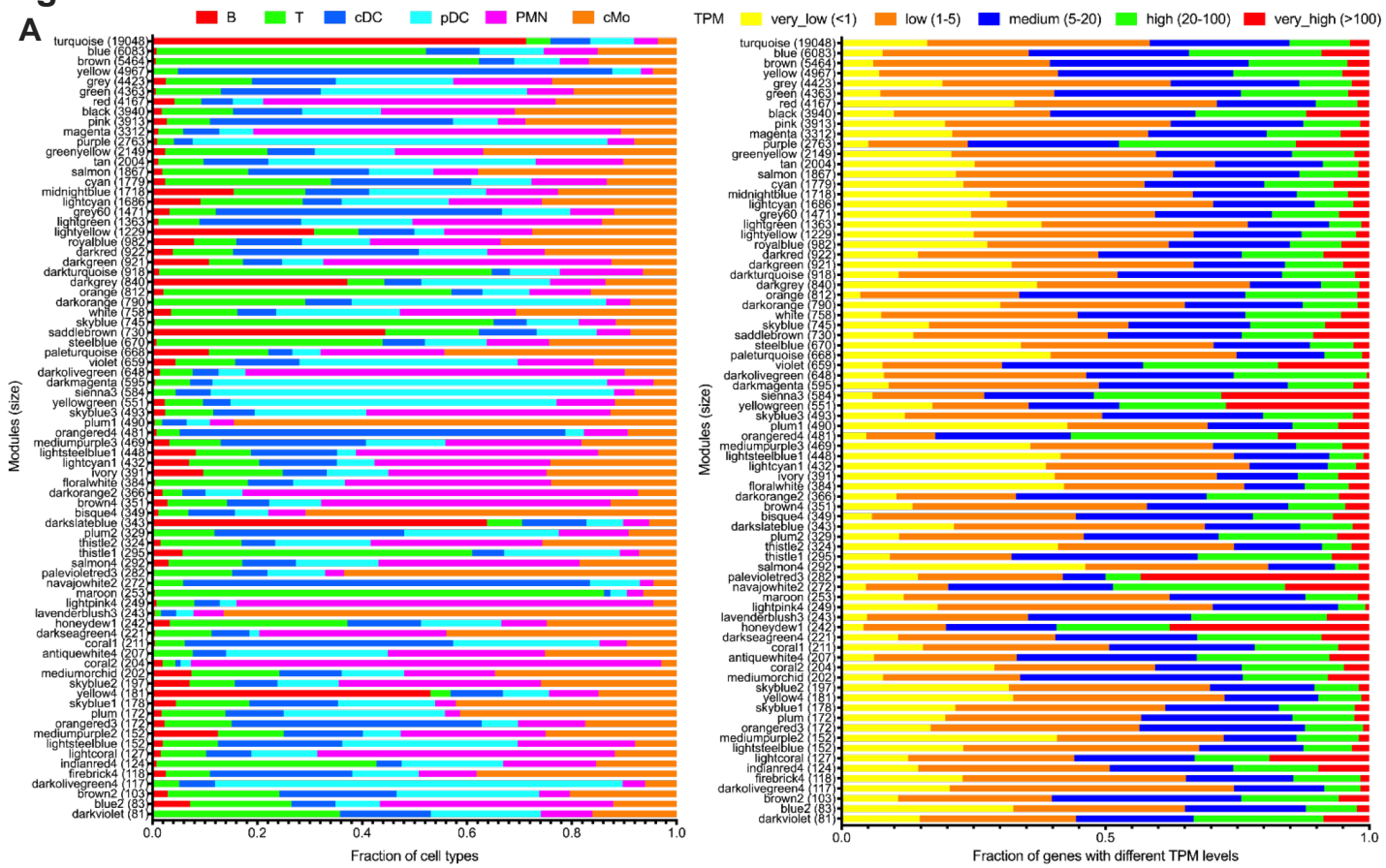
A
B
T
cDC
pDC
PMN
cMo
Modules (size)
Fraction of cell types
B
TPM
very_low (<1)
low (1-5)
medium (5-20)
high (20-100)
very_high (>100)
Modules (size)
Fraction of genes with different TPM levels

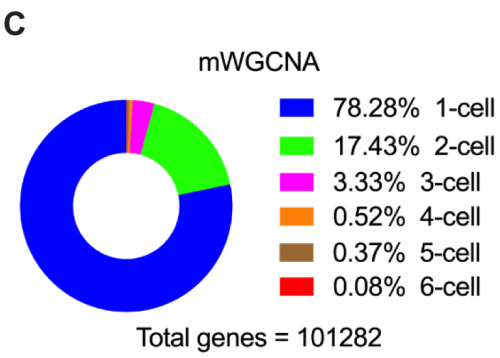
C
mWGCNA
78.28% 1-cell
17.43% 2-cell
3.33% 3-cell
0.52% 4-cell
0.37% 5-cell
0.08% 6-cell
Total genes = 101282

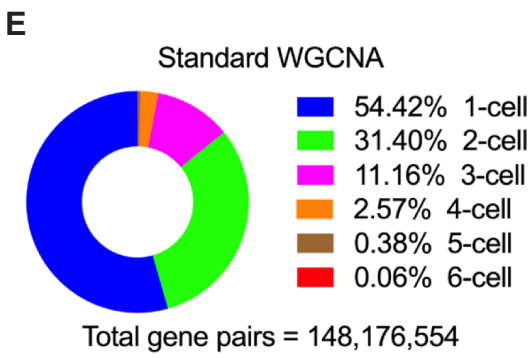
E
Standard WGCNA
54.42% 1-cell
31.40% 2-cell
11.16% 3-cell
2.57% 4-cell
0.38% 5-cell
0.06% 6-cell
Total gene pairs = 148,176,554

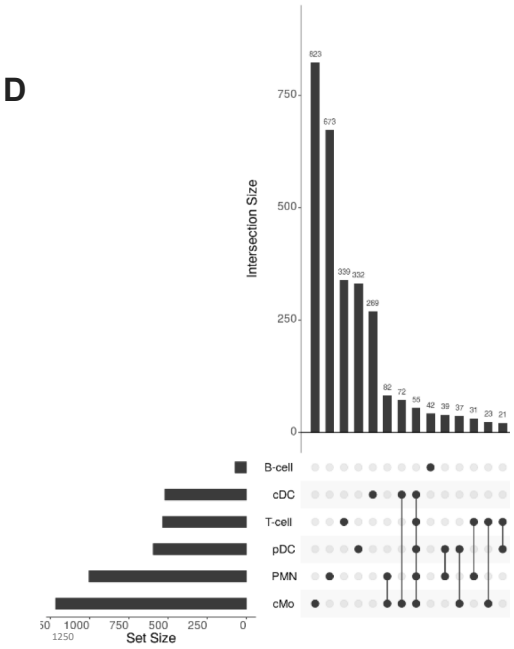
D
Intersection Size
B-cell
cDC
T-cell
pDC
PMN
cMo
Set Size

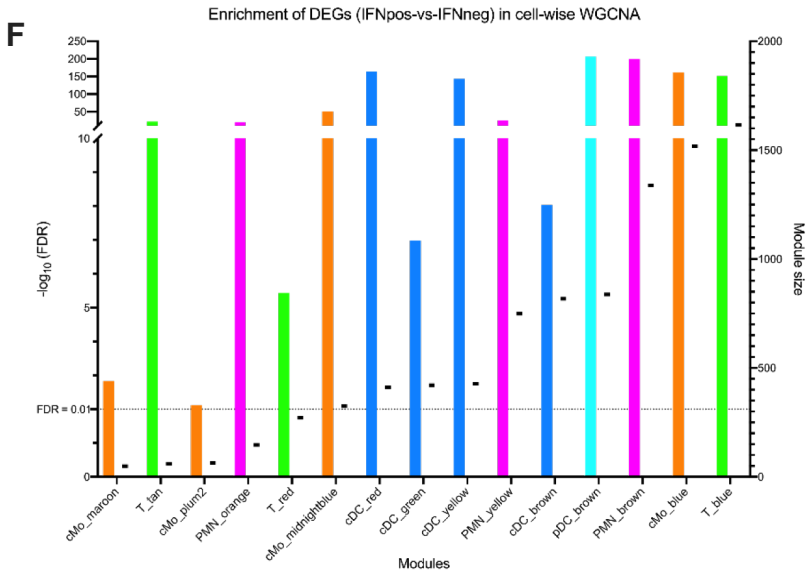
F
Enrichment of DEGs (IFNpos-vs-IFNneg) in cell-wise WGCNA
-log10 (FDR)
FDR = 0.01
Module size
Modules
cMo_maroon
T_tan
cMo_plum2
PMN_orange
T_red
cMo_midnightblue
cDC_red
cDC_green
cDC_yellow
PMN_yellow
cDC_brown
pDC_brown
PMN_brown
cMo_blue
T_blue

Supplemental Figure S6. Proportion of multi-genes in mWGCNA and gene-pairs in standard WGCNA from different cell types. (A) The figure depicts the mWGCNA analysis using combined transcriptomes from six different cell types. The mWGCNA has generated 78 different modules and a stacked column graph shows the proportion of genes from 6 different cell types in each module. The Y-axis shows all modules and the X-axis is the fraction of total number of genes in the corresponding modules. Gene numbers from different cell types are displayed in different colors as depicted in the cartoon. **(B)** The figure depicts the different gene expression levels (based on TPM) in mWGCNA analysis using combined transcriptomes from six different cell types. The mWGCNA has generated 78 different modules and a stacked column graph shows the proportion of genes from 5 different expression levels (very high, high, medium, low, and very low) in each module. The Y-axis shows all modules and the X-axis is the fraction of genes with different TPM levels in the corresponding modules. Different expression levels are displayed in different colors as depicted in the cartoon. **(C)** The donut chart shows the proportion of number of genes from different cell-types in mWGCNA. In this 78.28%, 17.43%, 3.33%, 0.52%, 0.37%, and 0.08% genes are coming from one, two, three, four, five, and six different cell types respectively. **(D)** The UpSetR plot shows the proportion of number of genes from different cell-types in the black module of mWGCNA. We only show sets with a minimum of 20 genes. **(E)** The donut chart shows the proportion of different gene-pairs in standard WGCNA from different cell types. Where 54.42%, 31.40%, 11.16%, 2.57%, 0.38%, and 0.06% gene pairs come from one, two, three, four, five, and six different cell types respectively. **(F)** Plot of selected 15 modules (from standard WGCNA of cell-types) that have significant enrichment of DEGs (IFNpos-vs-IFNneg) for that particular cell type. The X-axis shows modules with their enrichment in each cell type and Y1-axis shows $-Log_{10}$ value of FDR (based on hypergeometric test). Modules are sorted based on their increasing module size (shown as black dash on the Y2-axis).

Figure S7

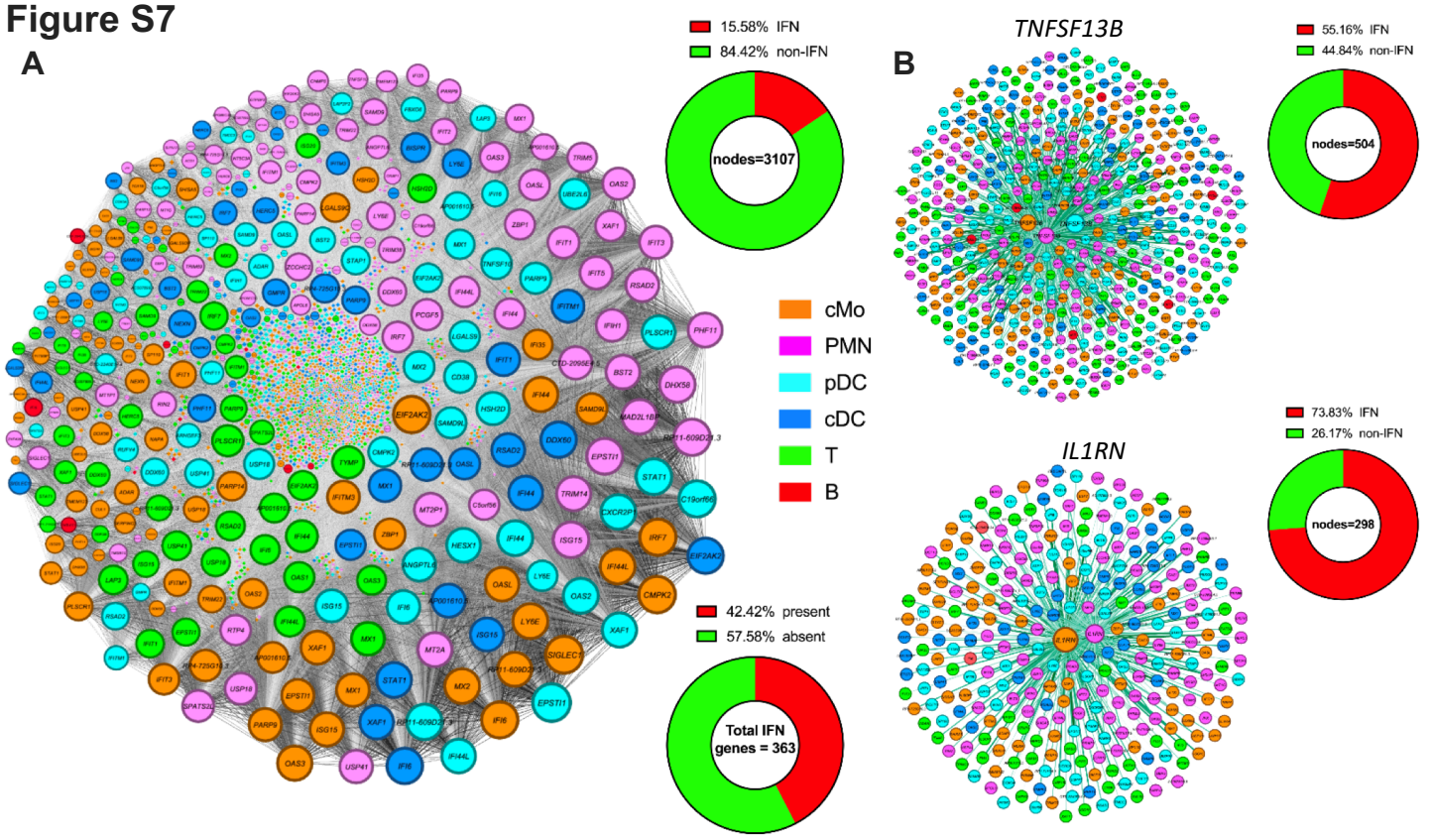
A
15.58% IFN
84.42% non-IFN
nodes=3107
cMo
PMN
pDC
cDC
T
B
42.42% present
57.58% absent
Total IFN genes = 363
B
TNFSF13B
55.16% IFN
44.84% non-IFN
nodes=504
IL1RN
73.83% IFN
26.17% non-IFN
nodes=298
Edge weight threshold >0.05

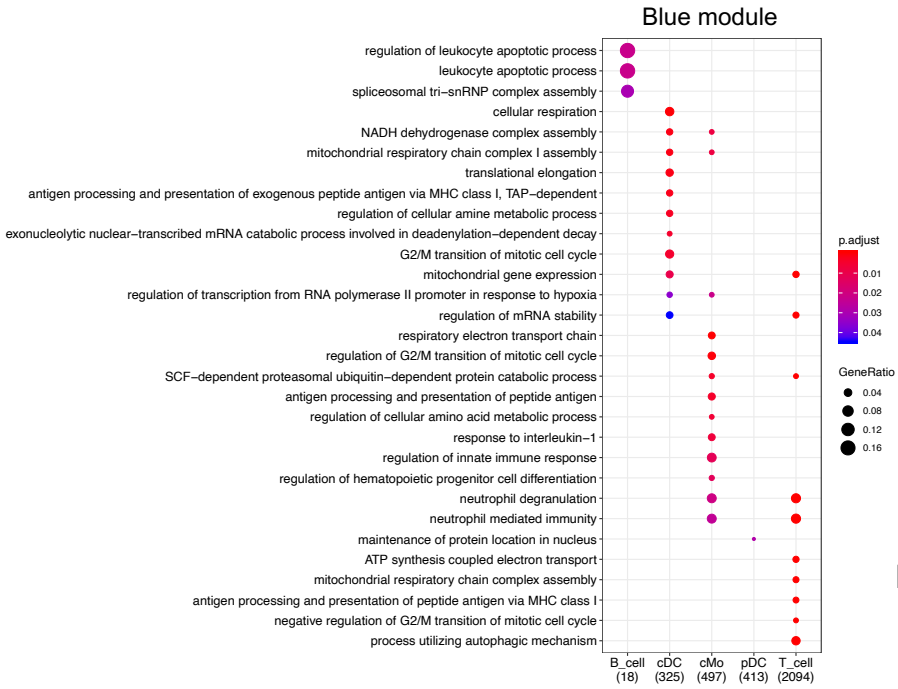
C
Blue module
regulation of leukocyte apoptotic process
leukocyte apoptotic process
spliceosomal tri−snRNP complex assembly
cellular respiration
NADH dehydrogenase complex assembly
mitochondrial respiratory chain complex I assembly
translational elongation
antigen processing and presentation of exogenous peptide antigen via MHC class I, TAP−dependent
regulation of cellular amine metabolic process
exonucleolytic nuclear−transcribed mRNA catabolic process involved in deadenylation−dependent decay
G2/M transition of mitotic cell cycle
mitochondrial gene expression
regulation of transcription from RNA polymerase II promoter in response to hypoxia
regulation of mRNA stability
respiratory electron transport chain
regulation of G2/M transition of mitotic cell cycle
SCF−dependent proteasomal ubiquitin−dependent protein catabolic process
antigen processing and presentation of peptide antigen
regulation of cellular amino acid metabolic process
response to interleukin−1
regulation of innate immune response
regulation of hematopoietic progenitor cell differentiation
neutrophil degranulation
neutrophil mediated immunity
maintenance of protein location in nucleus
ATP synthesis coupled electron transport
mitochondrial respiratory chain complex assembly
antigen processing and presentation of peptide antigen via MHC class I
negative regulation of G2/M transition of mitotic cell cycle
process utilizing autophagic mechanism
B_cell (18)
cDC (325)
cMo (497)
pDC (413)
T_cell (2094)
p.adjust
0.01
0.02
0.03
0.04
GeneRatio
0.04
0.08
0.12
0.16

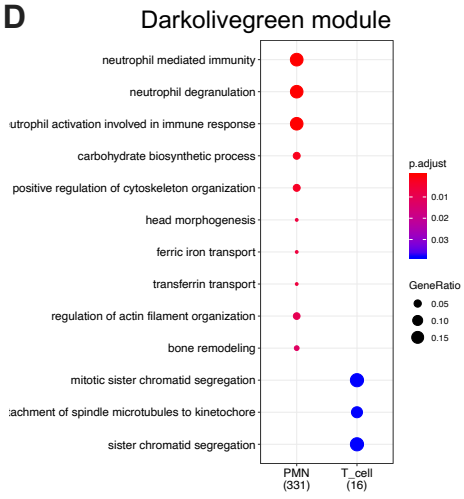
D
Darkolivegreen module
neutrophil mediated immunity
neutrophil degranulation
utrophil activation involved in immune response
carbohydrate biosynthetic process
positive regulation of cytoskeleton organization
head morphogenesis
ferric iron transport
transferrin transport
regulation of actin filament organization
bone remodeling
mitotic sister chromatid segregation
achment of spindle microtubules to kinetochore
sister chromatid segregation
PMN (331)
T_cell (16)
p.adjust
0.01
0.02
0.03
GeneRatio
0.05
0.10
0.15

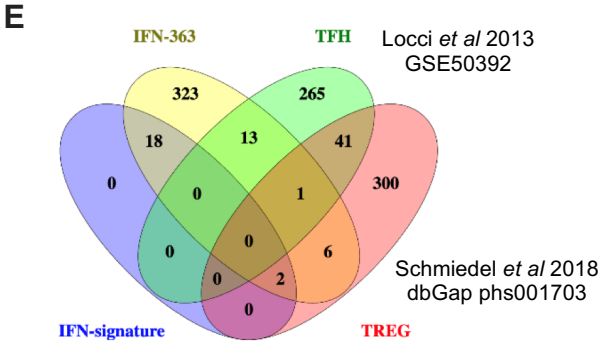
E
IFN-363
TFH
IFN-signature
TREG
323
265
18
13
41
0
0
1
300
0
0
6
0
2
0
Locci et al 2013
GSE50392
Schmiedel et al 2018
dbGap phs001703

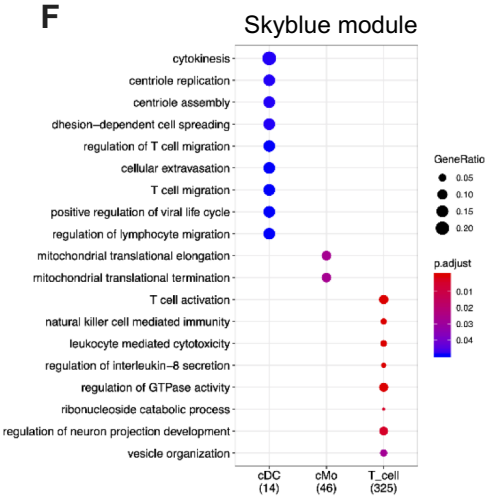
F
Skyblue module
cytokinesis
centriole replication
centriole assembly
dhesion−dependent cell spreading
regulation of T cell migration
cellular extravasation
T cell migration
positive regulation of viral life cycle
regulation of lymphocyte migration
mitochondrial translational elongation
mitochondrial translational termination
T cell activation
natural killer cell mediated immunity
leukocyte mediated cytotoxicity
regulation of interleukin−8 secretion
regulation of GTPase activity
ribonucleoside catabolic process
regulation of neuron projection development
vesicle organization
cDC (14)
cMo (46)
T_cell (325)
GeneRatio
0.05
0.10
0.15
0.20
p.adjust
0.01
0.02
0.03
0.04

Supplemental Figure S7. Multi cell type WGCNA (mWGCNA) reveals IFN-driven cross-talk between T cells and B cells. (A) The network of the black module genes visualized by Gephi. The nodes are colored according to cell of origin and sized according to the number of edges (connections), and the edge thickness is proportional to the strength of co-expression. The top donut chart shows that 15.58% nodes are IFN-related genes (from IFN-363) and the bottom donut plot shows that 42.42% of IFN-363 genes, from at least one-cell type, are present in the black module. **(B)** The Gephi based visualization of *TNFSF13B* (*BAFF)* (top) and *IL1RN* (bottom) connected genes in the black module and the corresponding donut chart show the proportion of IFN and non-IFN related nodes (based on IFN-363 genes). *TNFSF13B* from three different cell types (cMo, PMN, and pDC) and *IL1RN* from cMo and PMN are present in the black module. **(C-E)** Functional annotations (generated by clusterProfiler) of genes from each cell type in the blue **(C),** darkolivegreen **(D)** modules. The color shows the significance (in terms of P.adj) and the size is gene ratio of annotations. **(E)** A Venn diagram shows the overlap of TFH and TREG signature genes with IFN-20 and IFN-363 genes. We only used genes that are exclusively present in TFH (265) and TREG (300) signatures. **(F)** Similar plot to **(C-D)** but for the skyblue module.

Figure S8

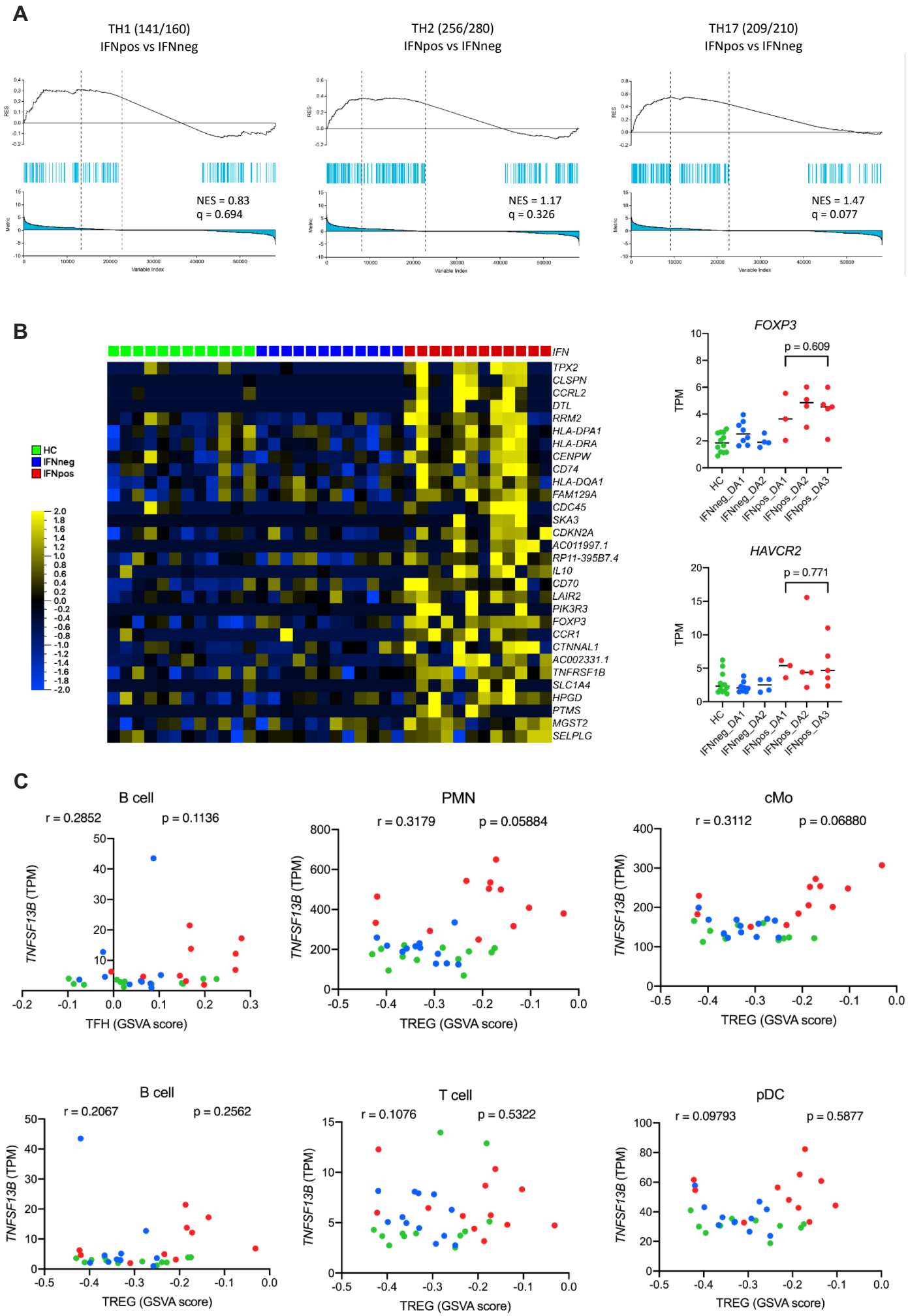
A
TH1 (141/160)
IFNpos vs IFNneg
NES = 0.83
q = 0.694
TH2 (256/280)
IFNpos vs IFNneg
NES = 1.17
q = 0.326
TH17 (209/210)
IFNpos vs IFNneg
NES = 1.47
q = 0.077
B
IFN
HC
IFNneg
IFNpos
TPX2
CLSPN
CCRL2
DTL
RRM2
HLA-DPA1
HLA-DRA
CENPW
CD74
HLA-DQA1
FAM129A
CDC45
SKA3
CDKN2A
AC011997.1
RP11-395B7.4
IL10
CD70
LAIR2
PIK3R3
FOXP3
CCR1
CTNNAL1
AC002331.1
TNFRSF1B
SLC1A4
HPGD
PTMS
MGST2
SELPLG
FOXP3
p = 0.609
TPM
HC
IFNneg_DA1
IFNneg_DA2
IFNpos_DA1
IFNpos_DA2
IFNpos_DA3
HAVCR2
p = 0.771
TPM
C
B cell
r = 0.2852
p = 0.1136
TNFSF13B (TPM)
TFH (GSVA score)
PMN
r = 0.3179
p = 0.05884
TNFSF13B (TPM)
TREG (GSVA score)
cMo
r = 0.3112
p = 0.06880
TNFSF13B (TPM)
TREG (GSVA score)
B cell
r = 0.2067
p = 0.2562
TNFSF13B (TPM)
TREG (GSVA score)
T cell
r = 0.1076
p = 0.5322
TNFSF13B (TPM)
TREG (GSVA score)
pDC
r = 0.09793
p = 0.5877
TNFSF13B (TPM)
TREG (GSVA score)

Supplemental Figure S8. TFH and TREG signatures are more enriched in IFNpos patients and *TNFSF13B* expression in multiple cell types correlates with TFH feature. (A) GSEA of TH1 (left), TH2 (middle), and TH17 (right) in the transcriptome of IFNpos versus IFNneg in T cells, presented as running enrichment score (RES) for the gene set, from most over-represented genes at left to most under-represented at right; values above the plot represent the normalized enrichment score (NES) and false discovery rate (FDR)-corrected significance value; Kolmogorov-Smirnov test. **(B)** A heatmap (left) shows expression of the top 30 TREG-related genes, where each gene is presented as row-wise z-scores of TPM values in IFNpos (red), IFNneg (blue) and HC (green); each column represents an individual patient. Individual expression plots (right) of two TREG related genes (*FOXP3* and *HAVCR2*) using IFN response status as well as SLEDAI categories. The provided p-values are based on unpaired *t*-test. **(C)** The correlation between GSVA score of TFH and TREG gene set and expression (TPM values) of *TNFSF13B* from different cell types. The Spearman's correlation with significance value (p-value) is given.

Figure S9

A Gating Strategy for TREG and TFH

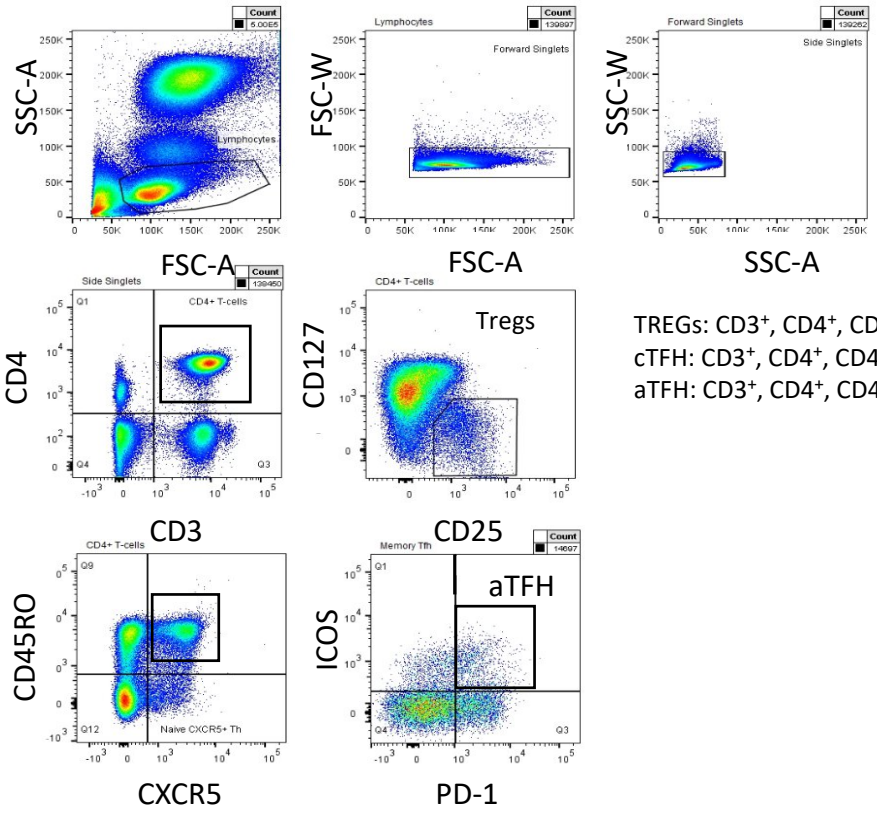

TREGs: $CD3^{+}$, $CD4^{+}$, $CD25^{+}$, $CD127^{low}$
cTFH: $CD3^{+}$, $CD4^{+}$, $CD45RO^{+}$, $CXCR5^{+}$
aTFH: $CD3^{+}$, $CD4^{+}$, $CD45RO^{+}$, $CXCR5^{+}$, $PD\text{-}1^{+}$, $ICOS^{+}$

B Gating Strategy for Plasma Cells and Plasmablasts

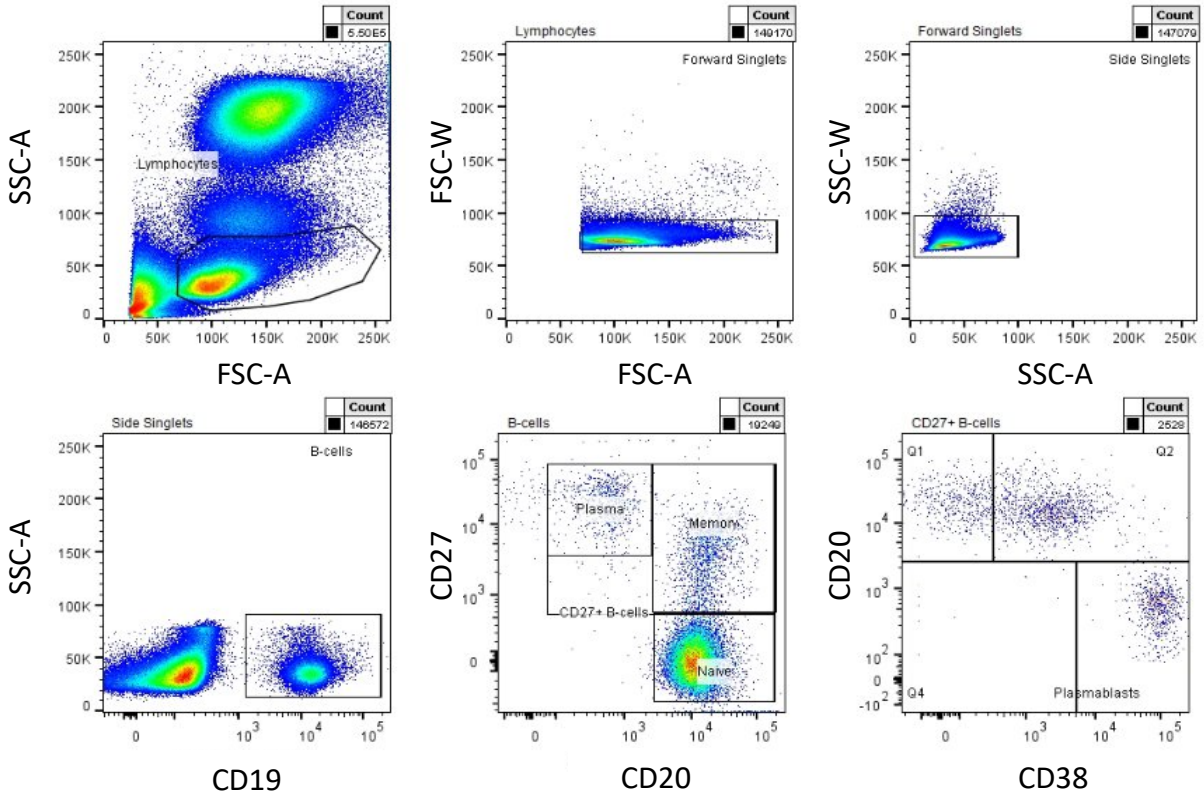

Supplemental Figure S9. Flow cytometry gating strategies. (A) Gating scheme of whole blood used for determination of the frequency of TREG, circulating (cTFH), and activated T follicular helper (aTFH) cells. Live lymphocytes were gated based on their forward side scatter versus side scatter profile followed by single cells gating by FSC then SSC and then finally according to their cell surface phenotype as follows. TREGs ($CD3^+$, $CD4^+$, $CD25^+$ $CD127^{low}$), circulating TFH (cTFH) ($CD3^+$, $CD4^+$, $CXCR5^+$, $CD45RO^+$), and activated circulating TFH (aTFH) ($CD3^+$, $CD4^+$, $CXCR5^+$, $CD45RO^+$, $PD\text{-}1^+$, $ICOS^+$). **(B)** Gating scheme of whole blood used for determination of the frequency of plasma cells and plasmablasts. Live lymphocytes were gated based on their forward side scatter versus side scatter profile followed by single cells gating by FSC then SSC and then finally according to their cell surface phenotype as follows. Plasma Cells ($CD19^+$, $CD20^-$, $CD27^+$ and plasmablasts ($CD19^+$, $CD20^-$, $CD27^+$, $CD38^+$).